

Nb/CuNi Sandwiches as Superconducting Spin-Valve Core Structures

A. Potenza and C. H. Marrows*

*School of Physics and Astronomy, E. C. Stoner Laboratory,
University of Leeds, Leeds. LS2 9JT United Kingdom*

(Dated: March 23, 2002)

We have investigated CuNi/Nb/CuNi trilayers, as have been recently used as the core structure of a spin-valve like device [J. Y. Gu et al., Phys. Rev. Lett. **89**, 267001 (2002)] to study the effect of magnetic configurations of the CuNi layers on the critical temperature, T_C , of the superconducting Nb. After reproducing a T_C shift of a few mK, we have gone on to explore the performance limits of the structure. The results showed the T_C shift we found to be quite close to the basic limits of this particular materials system. The ratio between the thickness and the coherence length of the superconductor and the interfacial transparency were the main features limiting the T_C shift.

PACS numbers: 74.78.-w, 72.25.Mk, 85.25.-j

Superconductor (S)/ferromagnet (F) proximity systems show many interesting physical effects originating from the coexistence of these two mutually exclusive orderings of matter¹. Ferromagnetism is expected to suppress superconductivity, as the presence of an exchange field breaks the time reversal symmetry of a Cooper pair. However, the splitting of the energy levels of the spin- \uparrow and spin- \downarrow electrons in the pair may not totally suppress the superconducting state. Exotic superconducting states, e.g. the Larkin-Ovchinnikov-Fulde-Ferrell (LOFF) state^{2,3}, can be adopted. In S/F multilayers, the mutual coexistence of the two effects is responsible for re-entrant superconductivity in the critical temperature (T_C) versus F thickness (d_m) behavior^{4,5}, and π -junction effects^{6,7}. Particularly interesting phenomena are predicted to happen in the limit of thin S layers, when the thickness d_s is comparable to the coherence length ξ_s . Non-local effects due to spatial variations in the exchange field over the coherence length will strongly affect the superconducting state. Therefore, it will be possible for a SC to distinguish between parallel (P) or antiparallel (AP) magnetic configurations in two adjacent F layers^{8,9}. In the latter case, the opposite orientations should partially cancel out, resulting in a much weaker effective field acting on the pair, and consequently a higher T_C .

This idea was the basis of a proposed model for a so-called superconducting spin-valve¹⁰, an F/S/F layer sequence where it is possible to switch between P and AP alignment of the two F layer moments. If the shift in critical temperature, ΔT_C , between the P ($T_{C,P}$) and AP ($T_{C,AP}$) configurations is bigger than the superconducting transition width, ΔW , then for $T_{C,P} < T < T_{C,AP}$, it is possible to valve the supercurrent by applying only a relatively small magnetic field to switch a soft F layer.

A first realization such a spin-switch has been reported, using CuNi for the F layers and Nb for the S spacer¹¹. Thin S layers are required, so the use of Nb and CuNi seems promising because of the very weak ferromagnetism of CuNi, which can allow the S layer to be far thinner if compared to systems with stronger ferromagnets such as Fe or Co. The device showed a small but measurable effect, with $\Delta T_C \approx 6$ mK, but this is still

much less than $\Delta W \approx 0.1$ K. Very recently this group has published a theoretical description of this structure¹². In the present Communication, we begin by reporting our results from a nominally identical sample, which reproduces just what was found in Ref. 11, confirming the existence of the superconducting spin-valve effect. Further results are then reported on the properties of Nb/CuNi trilayers, and the intrinsic limits in the device performance in this materials system are found by constraining as many parameters as possible experimentally, entirely using material grown in the same sputter chamber.

The samples, with planar dimensions of 10 mm \times 2 mm, were grown by dc magnetron sputtering on Si(100) substrates. The CuNi was sputtered from an alloy target, and characterized by vibrating sample magnetometry (VSM). The Curie temperature of a 5000 Å thick film, determined as the temperature where there is an upturn in the value of magnetic moment, was found to be ~ 40 K, which corresponds to a composition of ~ 51 atomic per cent Ni¹³, which compares well with 53 ± 2 atomic per cent Ni, determined by x-ray photoelectron spectroscopy. In the first set of samples, S1, spin-valve structures were grown with the layer sequence Ta/Ni₈₀Fe₂₀/CuNi/Nb/CuNi/Ni₈₀Fe₂₀/FeMn/Ta and the Nb thickness d_s varied, and 100 Å CuNi layers used. In S1, the core trilayer structure was embedded within two 30 Å Ni₈₀Fe₂₀ layers, as in Ref. 11, in order to improve the switching characteristics of the CuNi. The second set, S2, is a sequence of CuNi layers with thickness d_m increasing from 25 to 800 Å. The third set, S3, is composed of CuNi(100 Å)/Nb/CuNi(100 Å) trilayer structures with varying Nb layer thickness, and a Ta cap of ~ 30 Å. The last set, S4, consists of similar trilayers to S3, but with a Nb thickness of 230 Å varying CuNi thickness, and ~ 50 Å of Ge as a capping layer.

In Fig. 1 the hysteresis curves for the sample of S1 with $d_s=180$ Å are displayed for $T = 3$ K and $T = 2.5$ K, either side of the superconducting transition. At 3 K the magnetization reproduces a typical spin-valve behavior, where a region of AP alignment of the magnetic moments in the two F layers is distinguishable for $0 < \mu_0 H < 0.25$ T on the forward going branch of the curve.

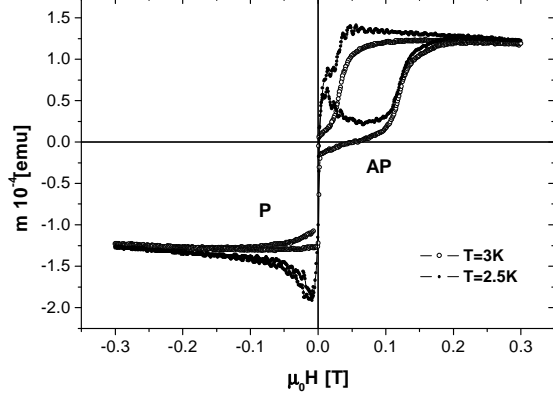


FIG. 1: Hysteresis loops for the 180Å Nb sample of the S1 set at temperatures just above (3 K) and just below (2.5 K) the critical temperature ($T_C \approx 2.8$ K).

The electrical resistance of the sample was measured by means of a low temperature dc 4-point probe in the *in-plane* geometry (probe spacing of 2.5 mm), where the external field is collinear to the sample length. Prior to the measurement for the superconducting transition (Fig. 2), a magnetic field of +0.5 T was applied. Subsequent application of small positive/negative external magnetic fields corresponds to switching between AP/P configurations by reversing the free layer only, in the usual spin-valve scheme. The resistance was then measured at alternating fields of ± 30 mT as the sample was cooled through the superconducting transition. Since these fields were equal and opposite, the direct effect of the applied field on the S layer is canceled out, as well as other effects of even symmetry such as magnetostriction in the F layers. We can see from Fig. 1 that our measurement fields are far from the coercivities of both magnetic layers, so that we can be confident that domain effects such as exchange field averaging¹⁴ and spontaneous vortex formation¹⁵ do not play any significant role. An averaging process over many consecutive readings was carried out, because of the changes of the resistance due to thermal fluctuations across the transition, reflected in the displayed error bars. In Fig. 2 the resistance vs. T plot for the sample shows the T_C split obtained by switching between P and AP alignment on F layers. The thickness of the Nb layer is nominally identical to the sample of Ref. 11 and the data are indeed very similar, showing a $T_C = 2.82$ K, a transition width $\Delta W \approx 0.1$ K and a $\Delta T_C \approx 2.5$ mK.

Theoretical predictions of ΔT_C are usually orders of magnitude larger. In order to find out more quantitatively the main limitations on performance, we carried out a series of experiments that were interpreted in terms of a theoretical model for the proximity effect by Tagirov¹⁰. Although this theory treats singlet pairing only, this is all that is required to deal with the collinear P and AP configurations that we concern ourselves with here¹⁶. This theory allows the calculation of the T_C of

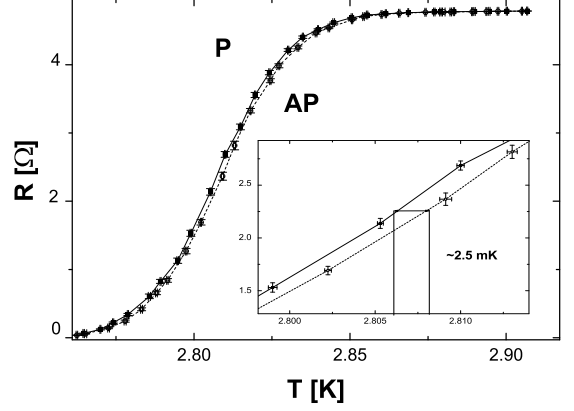


FIG. 2: Resistance vs. T plot close to T_C for the same sample (S1) as Fig. 1. The upper curve refers to P alignment (-30 mT), while the lower is for the AP case ($+30$ mT). The inset is a magnification showing a T_C shift of ~ 2.5 mK.

the F/SC/F trilayer (using Eqns. 8 and 9 of Ref. 10 for the P state, and 8 and 10 for the AP state) based on the values of four parameters:

$$\varepsilon = \sqrt{6} \frac{N_s \xi_s}{N_m \xi_I} \frac{2\pi T_0}{I}, \quad \mathfrak{T}_m, \quad \frac{\xi_I}{l_m}, \quad \frac{\xi_I}{d_m}. \quad (1)$$

$N_{s,m}$ are the densities of states at the Fermi energy in the S, F. ξ_s is the length scale of Cooper pairs in S in proximity systems (given by $\xi_s = \sqrt{D_s/2\pi T_{CS}}$ ¹⁷, with D_s the diffusion coefficient in the S and T_{CS} critical temperature of the bulk S). The magnetic stiffness length $\xi_I = \hbar v_m/2I$, where v_m is the Fermi velocity and I the exchange splitting in F. T_0 is the BCS critical temperature of the SC and \mathfrak{T}_m is the parameter accounting for the interface transparency¹⁸. l_m and d_m are the mean free path and the thickness of the F layer respectively. Our strategy was to fix as many as possible of these parameters with experimental values.

The resistivity as function of thickness d_m for the CuNi monolayers of S2 is plotted in the inset of Fig. 3(a), along with a fit to the Fuchs-Sondheimer relationship $\rho = \rho_B(1 + 3l_m/8d_m)$ where ρ_B is the bulk resistivity¹⁹. The fit yields $\rho_B = 57 \pm 1 \mu\Omega\text{cm}$ and $l_m = 44 \pm 2 \text{ Å}$. Resistance vs. T measured during cooling in zero field was used to determine T_C for the S3 set. The results are plotted in Fig. 3(b). A bulk T_C of ≈ 8 K for Nb can be observed, lower than the expected critical temperature of 9.2 K for pure Nb. The discrepancy is due to residual impurities and other defects found in thin film materials. In the limit of thin Nb layers, the proximity effect becomes larger, resulting in a falling T_C until a critical thickness $d_s^{\text{cr}} \approx 160 \text{ Å}$, below which superconductivity is totally suppressed. The previous result is consistent with reported data of Rusanov et al.⁷. The critical temperatures of the S1 samples are also plotted for comparison. The points fall on the same curve as for S3, thus show-

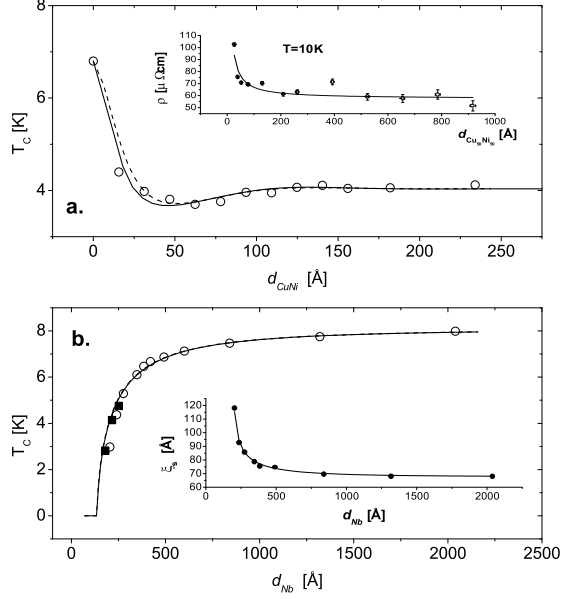


FIG. 3: (a) T_C vs. CuNi layer thickness, $d_{\text{CuNi}} (=d_m)$ for the S4 set. The lines are interpolated curves assuming $\pi T \ll I$ (solid) and in the general case (dashed), with parameters values of: $\xi_1/l_m=2.8$, $\xi_s/d_s=3.3$, $\mathfrak{T}_m=0.4, 0.45$ and $\varepsilon=1.9, 2.3$, respectively. In the inset the low temperature resistivity of $\text{Cu}_{50}\text{Ni}_{50}$ single layers is plotted vs. d_{CuNi} (S2 set of samples). (b) T_C vs. Nb layer thickness, $d_{\text{Nb}} (=d_s)$, in zero field cooling for the samples of the S3 (circles) and S1 (squares) sets, respectively. The lines are the same curves as in (a), plotted as a function of d_{Nb} , with $\xi_1/d_m=1.18$. Inset: ξ_s vs. d_s , the solid line is a fit of the data with the assumption of the scaling: $\xi_s \sim T_C^{-0.5}$.

ing that the layers outside the CuNi have no measurable effect on the superconductor. On the same S3 set, the coherence lengths in the out-of-plane field configuration were estimated. For this purpose, the critical fields, $H_{C\perp}$ vs. T were measured by sweeping H at fixed T and taking the value corresponding to half-height of the resistance transition, averaged over positive and negative fields. As predicted from Ginzburg-Landau (GL) theory, $H_{C\perp}$ goes linearly with T near T_C , because of the 3D behavior expected in perpendicular field configuration even for a thin film. From a linear fit of the curves near T_C , it is possible to extract the values of the GL perpendicular coherence length ξ_{GL} by means of the relationship:

$$H_{C\perp} = \frac{\phi_0}{2\pi(\xi_{\text{GL}})^2} \left(1 - \frac{T}{T_C}\right)^2 \quad (2)$$

where ϕ_0 is the flux quantum. ξ_s is related to ξ_{GL} by simple proportionality^{20,21}, $\xi_s=(2/\pi)\xi_{\text{GL}}$.

From the inset of Fig. 3(b), the value of ξ_s can be obtained in the limit of thick Nb as $\xi_s=70$ Å. The diagram also shows a divergent behavior of ξ_s in the opposite limit of thin Nb. This can be understood within

the framework of the de Gennes-Werthamer theory of the proximity effect²², where the coherence length of Cooper pairs in S is calculated as proportional to $(\gamma_e T_C/\sigma)^{-0.5}$, where σ is the electrical conductivity and γ_e is the coefficient of the electronic specific heat. The solid line in the inset of Fig. 3(b) is a fit corresponding to the behavior $\xi_s \propto T_C(d_s)^{-0.5}$. By using $\rho_{\text{Nb}} \approx 15 \mu\Omega\text{cm}$, a value of $5.9 \text{ mJ mol}^{-1} \text{ K}^{-2}$ for γ_e was calculated from the fit, which is acceptably close to the known value for Nb of $7.8 \text{ mJ mol}^{-1} \text{ K}^{-2}$, given the approximations we have made.

The T_C vs. d_m dependence for the S4 samples is plotted in Fig. 3(a). The samples are now capped with Ge instead of Ta to avoid proximity with nonmagnetic metals for thin F layers. A clear dip appears at $d_m \approx 60$ Å. This is in agreement with the data on Nb/CuNi bilayers reported in Ref. 24 (50 Å) and Ref. 7 (40 Å), where higher Ni concentrations have been used. The position of the minimum and ξ_1 are related through: $\xi_1 \approx 2d_m$ for $\mathfrak{T}_m > 5$ ²¹ and can be acceptably extended to lower \mathfrak{T}_m values, yielding in our case $\xi_1 \approx 120$ Å. The evaluation of l_m , d_m and ξ_1 allows us to fix the values of the last two parameters in (1): $\xi_1/l_m \simeq 2.8$ and $\xi_1/d_m \simeq 1.18$.

The remaining two parameters can be constrained by recalling that for F/S trilayers d_s^{cr} is related to \mathfrak{T}_m by²¹:

$$\frac{d_s^{\text{cr}}}{\xi_s} = 2\sqrt{2\gamma} \arctan\left(\frac{\pi}{\sqrt{2\gamma}} \frac{N_m v_m \xi_0}{N_s v_s} \frac{1}{\xi_s} \frac{1}{1 + (2/\mathfrak{T}_m)}\right), \quad (3)$$

with $\gamma \simeq 1.7811$ and ξ_0 the BCS coherence length in the S, given by $\xi_0 = (\hbar v_s)/(1.76\pi T_0)$. The latter relationship is valid in the limit of $d_m \gg \xi_1$, but it is still a very good approximation for $\mathfrak{T}_m < 1$ or, more generally, in the regime where T_C vs. d_m is nearly constant. By extracting N_s/N_m from (3) and substituting into ε as given in (1), we finally obtain:

$$\varepsilon \simeq \frac{3.9\pi}{\sqrt{\gamma}} \frac{1}{1 + (2/\mathfrak{T}_m)} \cot\left(\frac{d_s^{\text{cr}}}{2\sqrt{2\gamma}\xi_s}\right). \quad (4)$$

The set of free parameters (1) is then reduced to only the interface transparency \mathfrak{T}_m . The latter can be found by interpolating the data in Fig. 3(a), with the model of Ref. 18, and using for ε the values given by (4) as initial guesses. We then estimated $\mathfrak{T}_m \simeq 0.4$ and $\varepsilon \simeq 2$. In order to check the consistency of our results, we calculated the ratio N_s/N_m for bulk epitaxial $\text{Cu}_{50}\text{Ni}_{50}$ by means of the ASW software²⁵. By substituting $N_s/N_m \simeq 0.25$ into (1) and using the definition of ξ_1 and (3) we estimated $v_s \approx 3 \times 10^7 \text{ cm s}^{-1}$ and $2I = 1.8 \text{ meV}$. The value of v_s is fairly close to $2.77 \times 10^7 \text{ cm s}^{-1}$ quoted by Vodopyanov et al.²⁶, while the small exchange band splitting can be qualitatively justified with the low Curie temperature of the CuNi we used. This raises the concern that the low value of I brings the system close to the weak F/S limit ($I \lesssim \pi T$). In our case ($T \approx 4\text{K}$) we have $I \approx \pi T \approx 1 \text{ meV}$. The data of Fig. 3(a) were therefore interpolated within the same model extended to the low I region¹⁸, represented by the dashed line in Fig. 3(a). It is reassuring to note that the values of the set of parameters

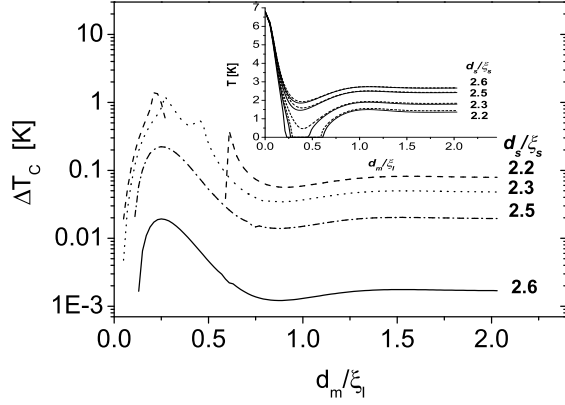


FIG. 4: T_C shift vs. d_m/ξ_I . The log scale is for better displaying the change of two orders of magnitude in the T_C shift with changing d_s/ξ_s . Inset: reduced T_C vs. d_m/ξ_I for the P (solid) and AP (dashed) cases used to calculate the shift in the main graph. The parameters values are $\xi_I/l_m=2.8$, $\mathfrak{T}_m=0.4$ and $\varepsilon=2$, which correspond to the measured values for Nb/CuNi systems.

1 came out to be approximately the same as within the previous approximation ($\varepsilon = 2.3$, $\mathfrak{T}_m = 0.45$), but the interpolation returned a higher value for I of 8 meV, incompatible with the weak F/S limit. This, coupled with the fact that the fitted curves are so similar, means that the concern is not a serious one.

In the theory of Fominov et al.²⁴ the parameter $\gamma_b = RA/\rho_f\xi_f$ (where R is the resistance of an interface of area A and ρ_f and ξ_f are the resistivity and coherence length of the ferromagnet, respectively) plays an analogous role to \mathfrak{T}_m in the Tagirov picture. By means of the Landauer formula²⁷, RA may directly linked to \mathfrak{T}_m yielding: $\gamma_b = 2l_m/3\mathfrak{T}_m\xi_f$ (the same relationship may be obtained directly by comparing Eqs. (8) and (14) in Ref. 24 with Eqs. (6) and (14) of Ref. 10, assuming a real valued diffusion coefficient). Our measured value of $\mathfrak{T}_m = 0.4$ gives $\gamma_b = 0.6$ when this formula is used. Fominov et al.²⁴ obtained a value of 0.3 when fitting their theory to unpublished Nb/CuNi bilayer data of Ryazanov. Both

measurements agree that the transparency of a CuNi/Nb interface is rather low.

The ΔT_C for Nb/CuNi systems can now be predicted as a function of the thickness of S and F layers. The results are summarized in Fig. 4. As expected, ΔT_C increases for smaller d_s/ξ_s , and has a clear maximum for $d_m/\xi_I \sim 0.25$. Actually, the real shift is strongly affected by proximity with the layer external to CuNi (mainly Py) for $d_m \leq \xi_I$, since ξ_I can be regarded as the coherence length of the injected pair in F¹⁰. In our case $\xi_I \approx 120$ Å so only the calculations with $d_m \gg \xi_I$ should be taken into account. This can probably explain why $\Delta T_C \approx 6$ mK in Ref. 11 is two orders of magnitude smaller than expected, for $d_m=50$ Å. The result is that in the best case of $d_s \approx d_s^{cr}$, the largest shift possible is $\Delta T_C = 0.4$ K. The maximum is accessible at temperatures lower than 1 K and rapidly falls to 0.05 K after $0.1d_s/\xi_s$, i.e. $d_s=7$ Å + d_s^{cr} . The region where the performance is enhanced is therefore hardly accessible.

We have shown, by a series of experimental measurements of the key physical parameters in the theory, that there are two main limitations of the CuNi/Nb system as the core of a superconducting spin-valve. These are the low value of interfacial transparency $\mathfrak{T}_m \approx 0.4$ (the same as for Pb/Fe systems²¹, but far lower than in Nb/Gd systems, where $\mathfrak{T}_m \approx 1.75$ ²⁶), and the high ratio d_s^{cr}/ξ_s which is roughly 2. It is desirable to have a superconducting layer that is much thinner than its coherence length, but this is not possible because of the extra pair breaking caused by the proximity effect in this system. By calculating the T_C shift with the thickness corresponding to the thinnest sample of S1, and considering an uncertainty of ± 5 Å in Nb thickness, we have $2.5 \leq d_s/\xi_s \leq 2.6$, which yields ΔT_C between 1 and 20 mK, in accordance to the shift of 2.5 mK we measured experimentally.

Acknowledgments

We would like to thank K. Critchley and S. D. Evans for assistance with the XPS measurements. This work was funded by the EPSRC, and by the EU via project NMP2-CT-2003-505587 “SFInX”.

* Electronic mail: c.marrows@leeds.ac.uk

¹ C. L. Chien and D. H. Reich, J. Magn. Magn. Mater **200**, 83 (1999).

² P. F. Fulde and R. A. Ferrel, Phys. Rev. **135**, A550 (1964).

³ A. I. Larkin and Y. N. Ovchinnikov, Sov. Phys. JETP **20**, 762 (1965).

⁴ C. Strunk, C. Sürgers, U. Pashen, and H. von Löhneysen, Phys. Rev. B **74**, 314 (1995).

⁵ J. S. Jiang, D. Davidović, D. H. Reich, and C. H. Chien, Phys. Rev. Lett. **77**, 1580 (1996).

⁶ T. Kontos, M. Aprili, J. Lesueur, and X. Grison, Phys. Rev. Lett. **86**, 304 (2001).

⁷ A. Rusanov, R. Bogaard, M. Hasselberth, H. Sellier, and J. Aarts, Physica C **369**, 300 (2002).

⁸ A. I. Buzdin, A. V. Vedyayev, and N. V. Ryzhanova, Europhys. Lett. **48**, 686 (1999).

⁹ R. Melin and D. Feinberg, Europhys. Lett. **65**, 96 (2004).

¹⁰ L. R. Tagirov, Phys. Rev. Lett. **83**, 2058 (1999).

¹¹ J. Y. Gu, C. Y. You, J. S. Jiang, J. Pearson, Y. B. Bazaliy, and S. D. Bader, Phys. Rev. Lett. **89**, 267001 (2002).

¹² C.-Y. You, Y. A. Bazaliy, J. Y. Gu, S.-J. Oh, L. M. Litvak, and S. D. Bader, Phys. Rev. B **70**, 014505 (2004).

¹³ P. A. Stampe and G. Williams, J. Phys.: Condens. Matter **10**, 6771 (1998).

- ¹⁴ A. Y. Rusanov, M. Hesselbeth, J. Aarts, and A. I. Buzdin, PRL **93**, 057002 (2004).
- ¹⁵ V. V. Ryazanov, V. A. Oboznov, A. S. Prokofiev, and S. V. Dubonos, JETP Lett. **77**, 39 (2003).
- ¹⁶ Y. V. Fominov, A. A. Golubov, and M. Y. Kupriyanov, JETP Lett. **77**, 609 (2003).
- ¹⁷ Z. Radović, L. Dobrosavljević-Grujić, I. Buzdin, and J. R. Clem, Phys. Rev. B **38**, 2388 (1988).
- ¹⁸ L. R. Tagirov, Physica C **307**, 145 163 (1998).
- ¹⁹ E. H. Sondheimer, Phys. Rev. **80**, 401 (1950).
- ²⁰ P. Koorevaar, Y. Suzuki, R. Coehoorn, and J. Aarts, Phys. Rev. B **49**, 441 (1994).
- ²¹ L. Lazar, K. Westerholt, H. Zabel, L. R. Tagirov, Y. V. Goryunov, N. N. Garif'yanov, and I. A. Garifullin, Phys. Rev. B **61**, 3711 (2000).
- ²² J. J. Hauser, H. C. Theuerer, and N. R. Werthamer, Phys. Rev. **142**, 118 (1966).
- ²³ C. Kittel, *Introduction to Solid State Physics* (John Wiley & Sons, New York, 1996).
- ²⁴ Y. V. Fominov, N. M. Chtchelkatchev, and A. A. Golubov, PRB **66**, 014507 (2002).
- ²⁵ J. Kübler, *Theory of Itinerant Electron Magnetism* (Oxford University Press, Oxford, 2000).
- ²⁶ B. P. Vodopyanov, L. R. Tagirov, H. Z. Durusoy, and A. V. Berezhnov, Physica C **366**, 31 42 (2001).
- ²⁷ R. Landauer, IBM J. Res. Dev. **1**, 223 (1957).